the FEBS Journal

Effects of a novel arginine methyltransferase inhibitor on T-helper cell cytokine production

Kevin Bonham[1], Saskia Hemmers[1], Yeon-Hee Lim[2], Dawn M. Hill[1], M. G. Finn[2] and Kerri A. Mowen[1]

1 Department of Chemical Physiology and Department of Immunology and Microbial Sciences, The Scripps Research Institute, La Jolla, CA, USA

2 Department of Chemistry and the Skaggs Institute for Chemical Biology, The Scripps Research Institute, La Jolla, CA, USA

Keywords

cytokines; inhibitors; nuclear factor of activated T cells interacting protein 45 kDa (NIP45); protein arginine methyltransferase; T-helper cell

Correspondence

Kerri A. Mowen, Department of Chemical Physiology, The Scripps Research Institute, 10550 North Torrey Pines Road, La Jolla, CA 92037, USA
Fax: +1 858 784 9190
Tel: +1 858 784 2248
E-mail: kmowen@scripps.edu
M. G. Finn, Department of Chemistry and the Skaggs Institute for Chemical Biology, La Jolla, CA 92037, USA
Fax: +1 858 784 8850
Tel: +1 858 784 2087
E-mail: mgfinn@scripps.edu

(Received 13 August 2009, revised 29 January 2010, accepted 22 February 2010)

doi:10.1111/j.1742-4658.2010.07623.x

The protein arginine methyltransferase (PRMT) family of enzymes catalyzes the transfer of methyl groups from *S*-adenosylmethionine to the guanidino nitrogen atom of peptidylarginine to form monomethylarginine or dimethylarginine. We created several less polar analogs of the specific PRMT inhibitor arginine methylation inhibitor-1, and one such compound was found to have improved PRMT inhibitory activity over the parent molecule. The newly identified PRMT inhibitor modulated T-helper-cell function and thus may serve as a lead for further inhibitors useful for the treatment of immune-mediated disease.

Structured digital abstract

- MINT-7710141: *Prmt1* (uniprotkb:Q63009) *physically interacts* (MI:0915) with *nip45* (uniprotkb:O09130) by *anti tag coimmunoprecipitation* (MI:0007)
- MINT-7710127: *Prmt1* (uniprotkb:Q63009) *physically interacts* (MI:0915) with *Prmt1* (uniprotkb:Q63009) by *anti tag coimmunoprecipitation* (MI:0007)

Introduction

Although the methylation of arginine residues has been recognized for more than four decades, the first mammalian protein arginine methyltransferase (PRMT) was cloned just over 10 years ago, in 1996 [1]. Since then, PRMTs have been shown to regulate transcription, protein and RNA subcellular localization, RNA splicing, DNA damage repair, and signal transduction [2]. Nine PRMT family members have been cloned and characterized to date, with putative 10th and 11th family members identified by homology searches [3]. Two types of PRMTs have been subclassified based on the symmetry of their reaction products. Using

Abbreviations

Adox, adenosine dialdehyde; AMI, arginine methylation inhibitor; IL, interleukin; GST, glutathione *S*-transferase; GST–GAR, GST fused to the glycine-rich and arginine-rich region of fibrillarin; IFN-γ, interferon-γ; NFAT, nuclear factor of activated T cells; MTA, methylthioadenosine; NIP45, NFAT interacting protein 45kDa; PMA, 4β-phorbol 12-myristate 13-acetate; PRMT, protein arginine methyltransferase; SAH, *S*-adenosylhomocysteine; SAM, *S*-adenosylmethionine; siRNA, small interfering RNA; Th, T helper; Th1, Type 1 T-helper; Th2, Type 2 T-helper; TK-Renilla luciferase, thymidine kinase promoter-driven Renilla luciferase.

S-adenosylmethionine (SAM) as the methyl donor, Type I PRMTs (1,3,4,6,8) catalyze asymmetric modification of arginine residues, depositing two methyl groups on a single guanidine nitrogen atom, and Type II PRMTs (5,7,9) perform symmetric transfer, placing one methyl group per terminal nitrogen of the arginine side chain. Both Type I and Type II PRMTs catalyze monomethylation as a reaction intermediate [4].

Post-translational modifications within T-cell-receptor signaling cascades allow T lymphocytes to initiate a rapid and appropriate immune response to pathogens. Indeed, co-engagement of the CD28 costimulatory receptor with the T-cell receptor increases PRMT activity and Vav1 methylation [5]. Perturbation of PRMT activity through the use of methylation inhibitors leads to diminished Vav1 methylation, as well as downstream interleukin (IL)-2 production [5]. PRMT5 promotes nuclear factor of activated T cells (NFAT)-driven promoter activity and IL-2 secretion [6]. Additionally, arginine methylation regulates cytokine gene transcription in T helper (Th) cells through arginine methylation of the NFAT cofactor, NFAT interacting protein 45 kDa (NIP45) [7]. These results demonstrate a role for arginine methylation in T-cell function, suggesting that PRMT inhibitors may be valuable for the treatment of autoimmune diseases.

As SAM is the methylation donor in the PRMT reaction, the use of SAM analogs is a logical strategy for the direct inhibition of PRMTs. As a SAM analog, sinefungin can compete for SAM binding and inhibit the activity of all SAM-dependent methyltransferases, including PRMTs [8]. Removal of the methyl group from SAM yields *S*-adenosylhomocysteine (SAH), which is broken down by SAH hydrolase [3]. SAH also acts as a methyltransferase inhibitor. Compounds such as (*Z*)-5′-fluoro-4′5′-didehydro-5′-deoxyadenosine (MDL 28,842) and adenosine dialdehyde (Adox), which hinder SAH hydrolase activity, cause an increase in SAH and thereby inhibit methylation [9]. Although methylthioadenosine (MTA) was reported to inhibit methyltransferase activity directly, it is an inefficient direct inhibitor of PRMT activity and is more likely to act via SAM catabolism [9–11]. Chemicals such as MDL 28,842, Adox, sinefugin and MTA are not specific to the PRMT pathways as they inhibit other SAM-dependent enzymes. Nonetheless, these inhibitors and similar molecules have been used widely in arginine methylation studies because of a lack of better reagents.

A non-nucleoside-specific small-molecule inhibitor of PRMTs, arginine methylation inhibitor (AMI)-1, was recently identified by Bedford and coworkers during screening of a commercial chemical library [8]. Other inhibitors have been discovered using virtual screening methods or by creating analogs to molecules in the original AMI-1 study, identifying a variety of potential PRMT inhibitory structures [12–15]. Our goal was to generate a less polar version of AMI-1 while maintaining PRMT inhibitor properties, hypothesizing that such a modification may enhance biological activity. We describe here the identification of one such compound and the characterization its inhibitory properties, focusing on its modulation of Th cell function.

Results

Chemistry

In the report disclosing the activity of AMI-1, Bedford and coworkers also identified the fluorescein triazine derivative AMI-6 as a selective arginine methyltransferase inhibitor, and the azo compound, AMI-9, as a significantly more potent, but unselective, inhibitor of both lysine and arginine methyltransferases (Fig. 1) [8]. In an effort to develop a more potent selective inhibitor, we melded elements of these two compounds. Accordingly, nonpolar functionality was conveyed to the aminonaphthol sulfonate core of AMI-1 by appending the azo moiety of AMI-9 to one side, giving compound **1**, and the dichlorotriazine group of AMI-6 to the other side, giving compound **4**. The Fmoc intermediate compound **2** was also tested, as were the isopropyl sulfonate esters, compounds **3** and **5**, to assay the importance of the sulfonate negative charge and the possibility of providing a nonpolar prodrug form of the active charged species (Fig. 1).

Characterization of PRMT inhibitors

To test the inhibitory activity of the compounds, we compared the ability of recombinant rat glutathione *S*-transferase (GST)–PRMT1 or recombinant human GST–PRMT4 to methylate histone 4 or histone 3, respectively, giving the IC_{50} values shown in Table 1. AMI-1 was a more effective inhibitor of PRMT1 than PRMT4 (Table 1). Compounds **1**, **2**, **4** and **5** inhibited both PRMT1 and PRMT4, with the latter enzyme being more sensitive to the added compounds. Comparisons between compounds **2** versus **3** and compounds **4** versus **5** demonstrated that the charged sulfonate group is advantageous. The triazine derivative compound **4** was most potent, with an IC_{50} of 4.15 μM for PRMT1 and an IC_{50} of 2.65 μM for PRMT4 (Table 1), similar to the reported IC_{50} value of 8.8 μM of the parent compound AMI-1 for human PRMT1. Further investigations focused on compound **4**.

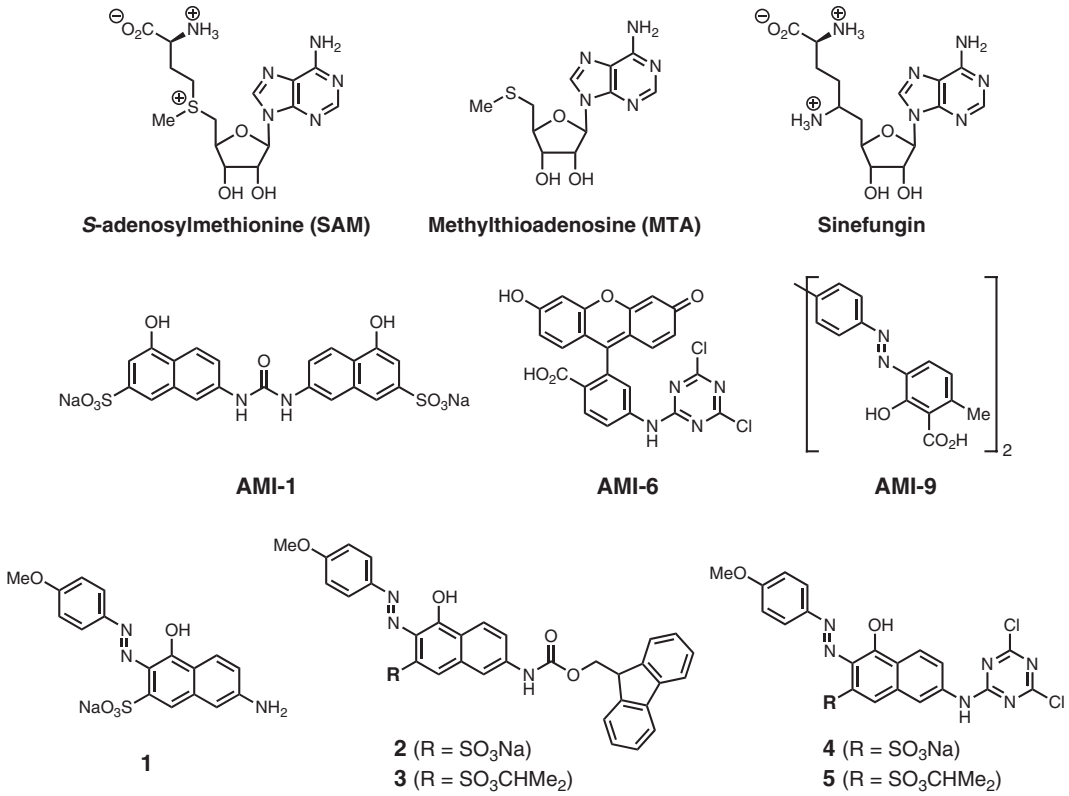

Fig. 1. Known PRMT inhibitors and compounds synthesized in this study. Chemical structures of SAM, MTA, sinefungin, AMI-1, AMI-6, AMI-9 and compounds **1**-**5**.

Table 1. Inhibition of histone methylation by PRMT1 and PRMT4 in the presence of the compounds depicted in Fig. 1.

Compound	PRMT1 IC_{50}	PRMT4 IC_{50}
AMI-1	8.8 μM[a]	169.8 ± 10.7 μM
1	397.3 ± 44.2 μM	196 ± 19.8 μM
2	332.5 ± 79 μM	56.1 ± 14.6 μM
3	No inhibition	No inhibition
4	4.15 ± 1.6 μM	2.65 ± 0.6 μM
5	56.7 ± 10.9 μM	52.4 ± 6.6 μM

[a] reported value using recombinant hPRMT1 and GST-Npl3 as substrate [8].

We determined the specificity of compound **4** by evaluating its effects on a panel of catalytically active recombinant Type I PRMTs using AMI-1 for comparison (Fig. 2A,B). Using *in vitro* methylation assays with increasing concentrations of inhibitory compounds, compound **4** proved effective against PRMT1, PRMT3 and PRMT4. The substrate identity influenced the inhibitory activity of AMI-1, which most potently inhibited PRMT1 methylation of GST–GAR (GST fused to the glycine-rich and arginine-rich region of fibrillarin) compared with histone 4 (Fig. 2A, top two panels). The published AMI-1 IC_{50} value for PRMT1 was determined using the glycine-rich and arginine-rich GST–Npl3 substrate [8]. Compound **4** prevented the methylation of GST–GAR by PRMT6 and PRMT8, while AMI-1 was less effective against these enzymes (Fig. 2B). Next, we examined the potency of compound **4** on Type II PRMTs. As the activity of recombinant PRMT5 is several hundred-fold lower than the activity of PRMT5 isolated from mammalian cells, we performed methyltransferase assays using PRMT5 immunoprecipitated from 293T cells. [16]. While compound **4** inhibited the activity of PRMT5, AMI-1 was ineffective as a PRMT5 inhibitor (Fig. 2C). In addition, compound **4** was selective for arginine methyltransferases over the SET domain-containing H3K4 lysine methyltransferase SET7/9, requiring at least 30-fold higher concentrations to inhibit recombinant SET7/9 activity relative to compound **4** inhibition of PRMT1 (Fig. 2A,C).

As SAM serves as the methyl donor in PRMT-dependent methylation reactions, we examined whether compound **4** inhibits PRMT activity by competing for SAM binding. Recombinant PRMT1 was incubated in the

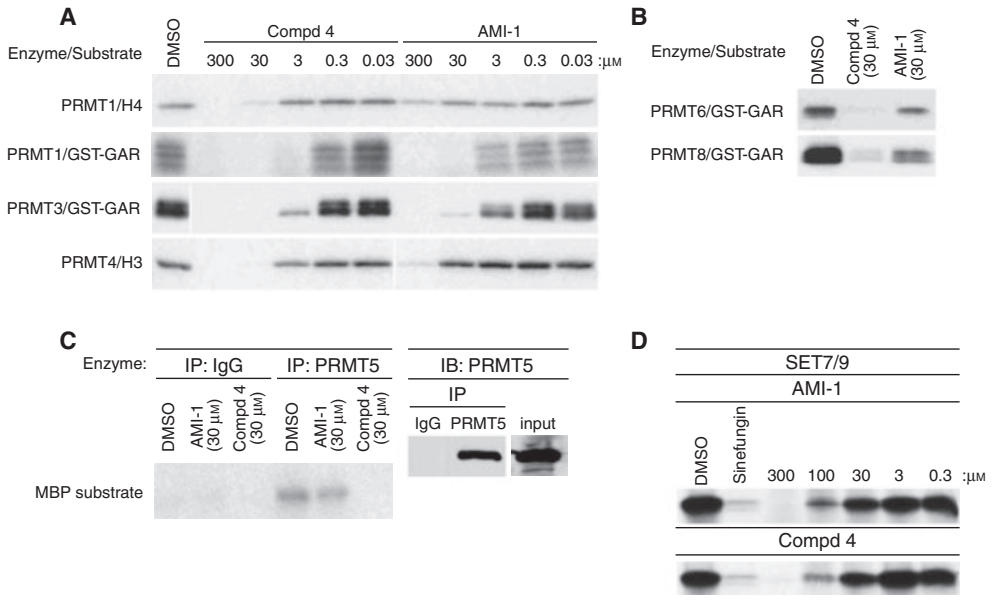

Fig. 2. Comparison of AMI-1 and compound 4 inhibitory activities. (A) *In vitro* methylation reactions of recombinant GST–PRMT1, GST–PRMT3 and GST–PRMT4 with the indicated substrate and [^{3}H]SAM in the presence of increasing concentrations of AMI-1 or compound **4** (Compd 4). (B) *In vitro* methylation reactions of recombinant GST–PRMT6 or GST–PRMT8 together with GST–GAR and [^{3}H]SAM in the presence of 30 μM AMI-1 or compound **4**. (C) Immunoprecipitated (IP) PRMT5 or isotype control from 293T-cell extracts was subjected to *in vitro* methylation reactions using the indicated concentrations of AMI-1 or compound **4** and MBP as substrate (left panel). Reaction inputs were determined by immunoblotting with PRMT5 antisera (right panel). (D) *In vitro* methylation reactions of recombinant Set7/9 with calf thymus histones as substrate and [^{3}H]SAM in the presence of increasing concentrations of AMI-1 or compound **4**. Data are representative of at least three independent experiments. DMSO, dimethylsulfoxide.

presence of radiolabeled SAM and a 50-fold molar excess of sinefungin, AMI-1, or compound **4**, followed by UV irradiation to cross-link the bound SAM to the protein. As previously published, the SAM analog, sinefungin, was competitive with SAM for binding, whereas AMI-1 was not [8]. Analysis by SDS/PAGE and visualization by fluorography (Fig. 3A) revealed that compound **4** did not block SAM binding to PRMT1.

PRMT1 has been shown to form dimers in crystal structure studies, and mutations within the dimerization interface reduce methyltransferase activity [4,17]. To test the possibility that compound **4** inhibits PRMT1 activity by preventing oligomerization, we performed co-immunoprecipitation experiments (Fig. 3B). Equal volumes of HA–PRMT1- and FLAG–PRMT1-transfected 293T-cell lysates were mixed and incubated with dimethylsulfoxide (lane 2), AMI-1 (100 μM (lane 3) or compound **4** (100 μM) (lane 4) during the co-immunoprecipitation. Specificity of the HA–PRMT1/FLAG–PRMT1 interaction was determined using an empty HA vector (Fig. 3B, lane 1). The presence of either compound did not interfere with the interaction between HA–PRMT1 and FLAG–PRMT1, indicating that compound **4** does not interfere with PRMT1 oligomerization.

To examine whether compound **4** is a reversible inhibitor, we performed washout experiments. Recombinant GST–PRMT1 bound to glutathionine beads was pre-incubated with compound **4** (100 μM) or AMI-1 (100 μM). The beads were then washed with methylation buffer only (Fig. 3C, indicated by '–') or with methylation buffer containing the indicated compound (Fig. 3C, indicated by '+') before methylation reactions using calf thymus histones as a source of the PRMT1 substrates histone 4 and histone 2A [18]. Inhibition by both compound **4** and AMI-1 was relieved by the washout, demonstrating that both are reversible PRMT inhibitors.

Biological activity

To determine whether compound **4** is cell permeable, we examined the effect of compound **4** on cellular PRMT activity. 293T cells were incubated with dimethylsulfoxide, compound **4**, or the general methylation inhibitor Adox [8]. Cell extracts were immunoblotted and incubated with an antibody recognizing H3R17 methylation (Fig. 4). Over this period no cellular toxicity with these treatments was observed (data not shown). At 100 μM, compound **4** induced more

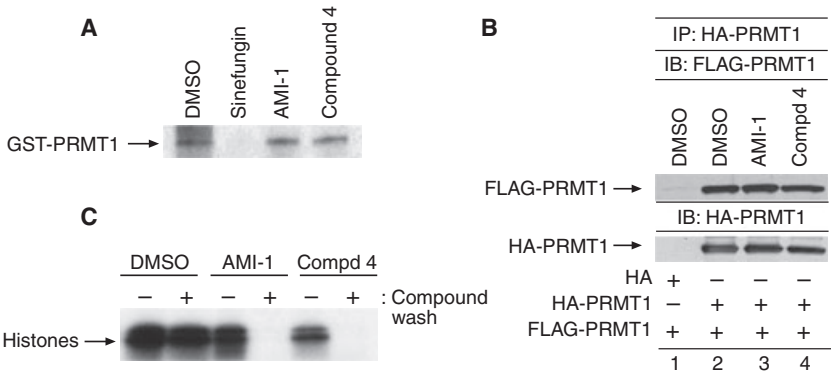

Fig. 3. Characterization of compound 4 inhibitory activity. (A) GST–PRMT1 was UV cross-linked to [^{3}H]SAM in the presence of dimethylsulfoxide (DMSO), sinefugin (100 μM), AMI-1 (100 μM) or compound **4** (100 μM), separated by SDS/PAGE and visualized by fluorography. (B) 293T cells were transfected with HA–PRMT1 or FLAG–PRMT1. Lysates from the FLAG–PRMT1 transfection were incubated with HA–PRMT1 immunoprecipitates (IP) in the presence of dimethylsulfoxide (lane 2), AMI-1 (100 μM, lane 3) or compound **4** (Compd 4) (100 μM, lane 4), resolved by SDS/PAGE and the immunoblot was incubated with an antibody to FLAG. Reprobing the immunoblot with an antibody to HA demonstrated equal loading. Specificity of the HA–PRMT1/FLAG–PRMT interaction was determined by incubating immunoprecipitates from vector-only transfected cells with FLAG–NIP45 lysates (C) Incubations of GST–PRMT1 glutathione beads with dimethylsulfoxide, AMI-1, or compound **4** were divided into two aliquots. Bead aliquots were washed in either the presence (+) or absence (–) of the indicated compounds. Washed aliquots were immediately subjected to *in vitro* methylation assays using calf thymus histones. Data are representative of three independent experiments.

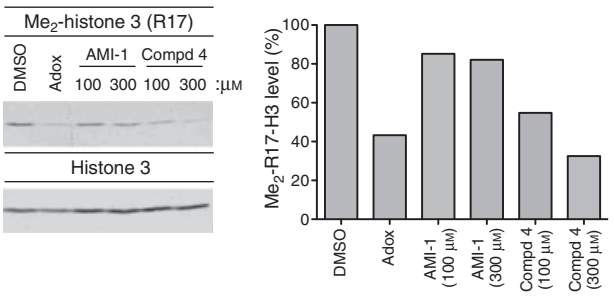

Fig. 4. Compound 4 is cell permeable. 293T cells were treated with dimethylsulfoxide (DMSO), AMI-1 (100 or 300 μM), compound **4** (Compd 4) (100 or 300 μM), or Adox (20 μM) for 24 h. Histone extracts were immunoblotted for H3R17 methylation (left panel). Quantification of the methylation levels of compound-treated samples relative to vehicle-treated samples is depicted in the right panel. Data are representative of three independent experiments.

than 40% reduction in H3R17 methylation, a significant increase in inhibitory activity relative to AMI-1.

Because compound **4** interferes with cellular PRMT activity, we examined its effects on PRMT-dependent gene regulation. Type 1 T-helper (Th1) cells modulate the immune response largely by the secretion of interferon-γ (IFN-γ), while type 2 T-helper (Th2) cells secrete IL-4 [19]. PRMTs have been shown to regulate Th-cell activation and cytokine secretion [5,7,20]. Indeed, PRMT1 augments both IFN-γ and IL-4 promoter activity, and general methylation inhibitors decrease IFN-γ and IL-4 transcript levels [7]. We examined the effect of compound **4** on the cytokine expression of Th1 and Th2 cells (Fig. 5). As shown previously, MTA diminished the production of both IFN-γ and IL-4 (Fig. 5A) [7]. Treatment with compound **4** reduced the production of IFN-γ from Th1 cells by more than 60% and the levels of IL-4 from Th2 cells by more than 75%, while incubation with AMI-1 reduced Th-cell cytokine expression by less than 40%. Compound **4** inhibited IFN-γ secretion by Th1 cells and IL-4 secretion by Th2 cells in a dose-dependent manner, with significant effects seen at 10 μM for IFN-γ secretion and at 0.1 μM for IL-4 secretion (Fig. 5B). Thus, IL-4 production is more sensitive than IFN-γ production to treatment with compound **4**. Importantly, compound **4** did not affect Th-cell viability (Table 2). Indeed, both AMI-1 and compound **4** enhanced Th-cell proliferation, the latter to a greater degree, suggesting a possible correlation between PRMT inhibition and T-cell proliferation, while MTA treatment inhibited T-cell proliferation (Fig. 5C). Thus, the reduced Th-cell cytokine expression following treatment with AMI-1 or compound **4** is not a result of increased cell death or reduced cell numbers.

As compound **4** is a cell-permeable PRMT inhibitor capable of modulating Th-cell cytokine secretion, it could suppress IL-4 levels by altering promoter activation or by affecting RNA stability. Accordingly, we tested the effect of compound **4** on the activity of a Th2 selective region of the IL-4 promoter (−760 to +68), which is responsive to transactivation by NFATc2 and

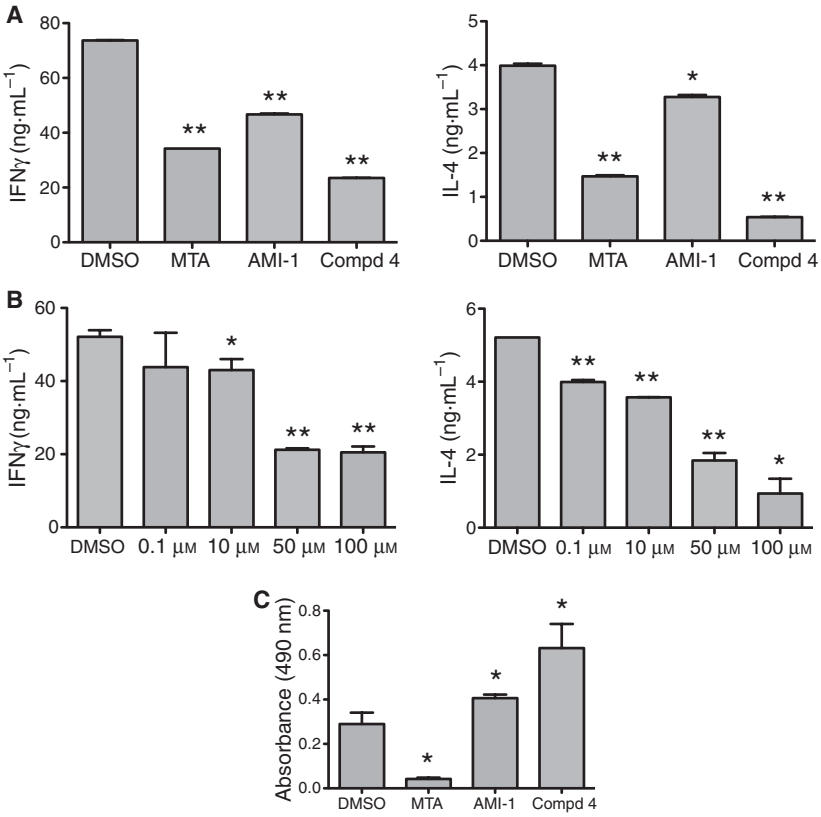

Fig. 5. Effects of compound 4 on Th cell function and proliferation. (A) Th1 cells or Th2 cells were stimulated with plate-bound anti-CD3 in the presence of dimethylsulfoxide (DMSO), MTA (100 μM), AMI-1 (100 μM) and compound **4** (Compd4) (100 μM). Supernatants were analyzed by ELISA to determine the production of IFN-γ by Th1 cells (left panel) or the production of IL-4 by Th2 cells (right panel). (B) Th1 cells or Th2 cells were stimulated with plate-bound anti-CD3 in the presence of dimethylsulfoxide or varying concentrations of compound **4**, and IFN-γ (left panel, Th1 cells) or IL-4 (right panel, Th2 cells) levels were determined by ELISA. (C) Th cells were stimulated with plate-bound anti-CD3 in the presence of dimethylsulfoxide, MTA, AMI-1, or compound **4**. Cellular proliferation was determined using the MTS [3-(4,5-dimethylthiazol-2-yl)-5-(3-carboxymethoxyphenyl)-2(4-sulfophenyl)-2H-tetrazolium] assay. $*P < 0.05$, $**P < 0.01$. Data are representative of at least three independent experiments.

Table 2. Viability of T helper cells in the presence of MTA or compound 4.

	Per cent viable	Per cent apoptotic	Per cent necrotic
Dimethylsulfoxide	95.9	2.2	2.0
MTA (100 μM)	90.9	4.9	4.2
cpd **4** (100 μM)	94.2	1.7	3.0

its binding partner NIP45 [21]. We transfected Jurkat cells, a human T-cell line that contains endogenous IL-4 promoter transactivating factors, with an IL-4 luciferase reporter. The transfected cells were incubated with dimethylsulfoxide, compound **4**, AMI-1 and Adox (Fig. 6A). As expected, Adox greatly diminished the promoter reporter activity of IL-4 [7]. Incubation with AMI-1 decreased the promoter activity, while compound **4** diminished the IL-4 promoter activity even further. Incubation with compound **3**, which did not exhibit *in vitro* PRMT inhibitory activity (Table 1), also did not interfere with IL-4 promoter activity (Fig. 6B). These data support the notion that the decrease in production of IL-4 by Th2 cells occurred, at least in part, at the transcriptional level.

The nuclear protein, NIP45, was isolated by virtue of its ability to interact with NFATc2 in a yeast two-hybrid screen [21]. NIP45 has been reported to combine with two critical Th2 transcription factors, c-Maf and NFATc2, to induce the expression of IL-4 in a normally non-IL-4-producing cell line [21]. NIP45 contains an arginine-rich amino terminus, which is a substrate of PRMT1. Arginine methylation facilitates the interaction between NIP45 and NFAT, thereby augmenting cytokine expression [7]. As a transcriptional co-activator, PRMT1 is recruited to the NFAT complex via NIP45, forming a tripartite complex that probably serves to enhance NFAT-driven transcriptional activity [7,22]. Inhibition of methyltransferase activity by MTA treatment diminished the PRMT1/NIP45 interaction [7]. To determine whether inhibition of PRMT activity by compound **4** would also disrupt the PRMT1/NIP45 association, 293T cells were transfected with HA–PRMT1 and FLAG–NIP45, and co-immunoprecipitation assays were performed. As predicted, Adox treatment reduced the association between PRMT1 and NIP45 compared to incubation with the compound vehicle dimethylsulfoxide (Fig. 6C, compare lanes 3 and 4). Additionally, both AMI-1 and compound **4** interfered with the NIP45 and PRMT1

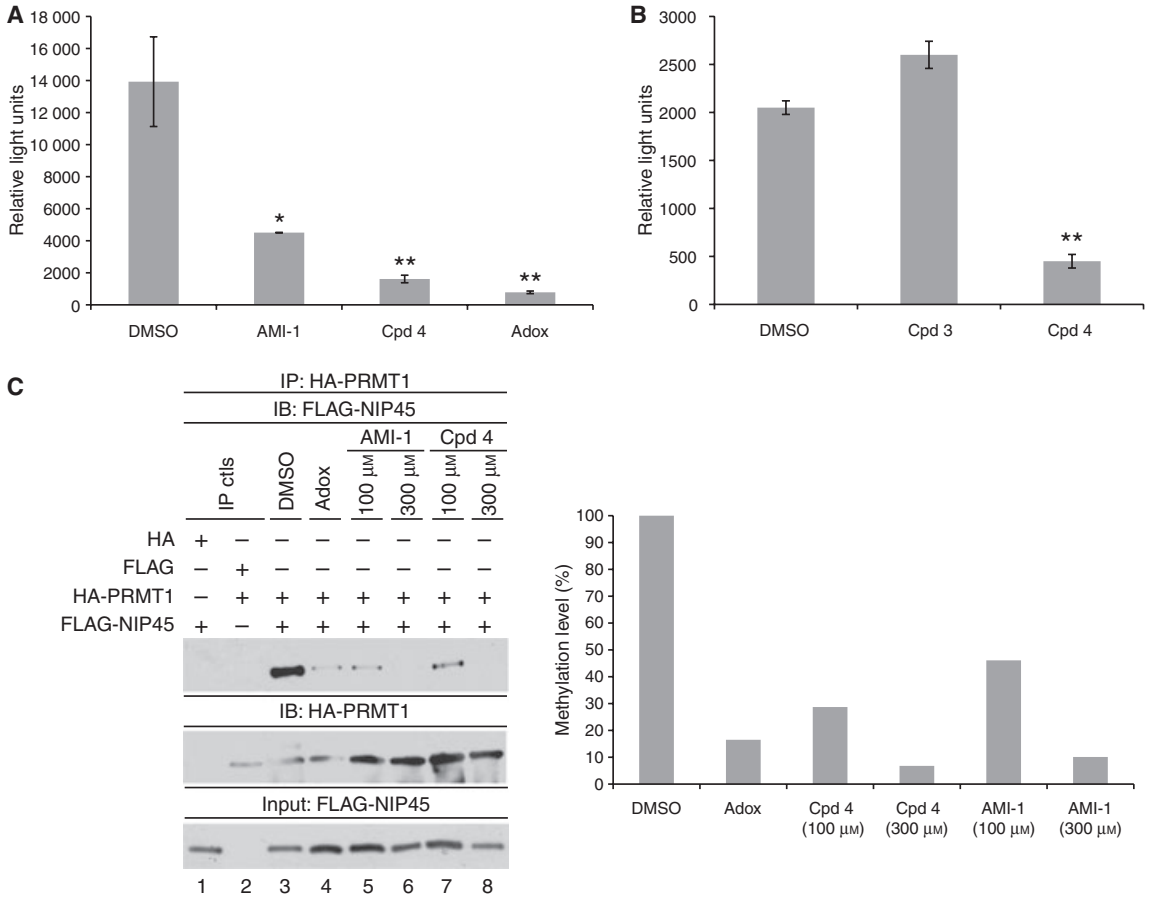

Fig. 6. Compound 4 inhibits IL-4 promoter activity and the interaction between NIP45 and PRMT1. (A) Jurkat cells were transfected with the IL-4 luciferase reporter (3 μg) along with the TK-Renilla luciferase vector (10 ng) as an internal control. Transfectants were pretreated with dimethylsulfoxide (DMSO), AMI-1 (100 μM), compound **4** (Cpd 4) (100 μM), or Adox (20 μM) for 18 h before stimulation for 6 h with PMA/ionomycin. Luciferase values were calculated relative to TK-Renilla luciferase internal controls. Similar results were obtained in at least three independent experiments. $*P < 0.05$, $**P < 0.01$. (B) The same procedure was followed as described for Fig. 6A except that cells were treated with compound **3** (Cpd 3) (100 μM) or compound **4** (100 μM). $**P < 0.01$. (C) 293T cells transfected with HA–PRMT1 and FLAG–NIP45 expression vectors were treated with dimethylsulfoxide (lane 3), Adox (20 μM, lane 4), AMI-1 (100 μM, lanes 5–6), or compound **4** (100 μM, lanes 7–8). Lysates were immunoprecipitated with anti-HA agarose, and immunoprecipitates were probed for FLAG–NIP45 using an antibody recognizing the FLAG epitope (top panel). HA–PRMT immunoprecipitate levels were evaluated by reblotting with an antibody to HA (middle panel). The bottom panel demonstrates FLAG–NIP45 input levels. Quantification of FLAG–NIP45/HA–PRMT association levels are depicted relative to the dimethylsulfoxide-treated sample (right panel). Data are representative of three independent experiments.

interaction, supporting the notion that both are bona fide arginine methyltransferase inhibitors (Fig. 6C, lanes 5–8). These data suggest that compound **4** may diminish the production of IL-4 by Th2 cells, at least in part, by interfering with the function of NIP45.

Discussion

Here, we have identified compound **4** as a selective PRMT inhibitor that targets both Type I and Type II PRMTs. The effectiveness of compound **4** on PRMT1 inhibition was dependent upon the substrate used, with methylation of GST–GAR being more responsive to inhibition than histone 4. A histone 4 and an arginine-rich and glycine-rich peptide were recently compared in kinetic studies with PRMT1. The K_m of the histone 4 peptide was about 10-fold lower than that of the arginine-rich and glycine-rich peptide, suggesting that the inhibition threshold may differ between PRMT1 substrates [10]. Compound **4** is a reversible inhibitor, limiting its *in vivo* toxicity. Also, compound **4** was mostly inactive against the lysine methyltransferase, Set7/9, in methylation assays. Importantly, compound **4** potently inhibited cellular H3R17 methylation, supporting the notions that compound **4** is cell permeable and is capable of inhibiting endogenous PRMT activity. It is

important to note that AMI-1 was first identified as an HIV-1 reverse transcriptase inhibitor [23]. Therefore, it will be important to determine whether compound **4**, as a derivative of AMI-1, is a selective inhibitor of endogenous PRMT activity.

The hybrid structure of compound **4** incorporates features of the AMI-1, AMI-6 and AMI-9 compounds described by Bedford and colleagues [8]. AMI-1, AMI-6 and AMI-9 were all effective methyltransferase inhibitors. Only AMI-1 and AMI-6 demonstrated selectivity for the PRMTs, although AMI-6 was minimally active against a cellular PRMT substrate [8]. Computational modeling suggested that AMI-1 spans the SAM-binding and arginine-binding pockets of PRMT1; however, AMI-1 did not compete for [^{3}H]SAM binding to recombinant PRMT1 [8,24]. Additionally, in a study using peptide-based fluorescent reporters, AMI-1 blocked PRMT1 binding to its substrate [25]. The mechanism of action of compound **4** is not completely clear, but it neither competed with SAM binding nor blocked PRMT1 dimerization.

In the first report of specific small-molecule PRMT inhibitors, Bedford and coworkers used an antibody-based high-throughput screening to identify several AMIs (Table 2) [8]. Of these, AMI-1 showed interesting selectivity by not inhibiting the lysine methyltransferase Set7/9 but was only weakly cell permeable, limiting its use *in vivo* [8]. In follow up studies, the bromo-moiety containing the AMI-5 structure was used as a template to create several new inhibitors with similar potency to AMI-1 (at low micromolar concentrations) [14,15]. Using 26 AMI analogs, one low-micromolar PRMT1 inhibitor was identified, and cellular activity was not reported [24]. Virtual ligand screening using the published PRMT1 structure has resulted in several novel compounds with inhibitory activity (thyglycolic amide, allantodapsone) [12,13]. Thompson and coworkers generated PRMT1 inhibitors using *in situ* bisubstrate generation (D2AAI), but none of these compounds was more potent than AMI-1 [26]. Recently, both Methylgene and Bristol-Myers Squibb have reported high-potency (picomolar IC_{50}) and selective PRMT4 inhibitors, although the Methylgene compound was not active in cellular assays and no cellular data were reported for the Bristol-Myers Squibb compounds [27–29]. Additionally, we found that while compound **4** inhibits both Type I and Type II PRMTs, AMI-1 distinguishes between the two PRMT subclasses. Thus, a variety of chemical structures can serve as PRMT inhibitors, and highly potent and selective PRMT structures are achievable.

The NFAT interacting protein, NIP45, is also a PRMT1 substrate [7]. Arginine methylation of NIP45 promotes NFAT-driven transcription [7]. In previous studies, we used MTA treatment to support a role for PRMTs in Th-cell cytokine expression [7]. Using compound **4**, we have extended these earlier studies, showing that methyltransferase inhibition results in the inhibition of IFN-γ and IL-4 production, interference with IL-4 promoter activity and impairment of the interaction between PRMT1 and NIP45.

Several lines of evidence strongly suggest that specific PRMT inhibitors may be valuable for the treatment of autoimmune diseases such as rheumatoid arthritis [5–7,30–33]. PRMTs modify and regulate several critical immunomodulatory proteins. Post-translational modifications within T-cell-receptor signaling cascades allow T lymphocytes to initiate a rapid and appropriate immune response to pathogens. Co-engagement of the CD28 costimulatory receptor with the T-cell receptor elevates PRMT activity and cellular protein arginine methylation, including methylation of the guanine nucleotide exchange factor Vav1 [5]. Incubation with MDL 28,842 diminished methylation of the guanine exchange factor, Vav1, as well as IL-2 production. Similarly, MTA treatment and small interfering RNA (siRNA) directed against PRMT5 both inhibited NFAT-driven promoter activity and IL-2 secretion [6]. We also demonstrated that arginine methylation of the NFAT cofactor, NIP45, within Th cells by PRMT1 promotes its association with NFAT, thereby driving NFAT-mediated cytokine gene expression [7]. In fibroblast cell lines, PRMT1 also co-operates with Carm1 to enhance nuclear factor-κB (NF-κB) p65-driven transcription and facilitate the transcription of p65 target genes such as tumor necrosis factor-α (TNF-α) [32]. Symmetric dimethylation of Sm D1 and D3 forms an epitope for the production of anti-Sm autoantibodies, which are often found in lupus [30,31,33]. Taken together, these results demonstrate an important role for arginine methylation in inflammation, suggesting that PRMT inhibitors may be valuable for the treatment of autoimmune diseases.

Inhibition of PRMT activity using AMI-1 or compound **4** augmented Th-cell proliferation. It will be important to determine whether compound **4** also enhances the proliferation of transformed cells. The combination of compound **4** treatment along with a PRMT siRNA approach may provide some insight into the mechanism behind this phenomenon. Because PRMT activity promotes Th-cell cytokine production, compound **4** and more potent derivatives thereof may be useful for treating Th-cell-driven autoimmune diseases, such as multiple sclerosis. Further work to develop more potent derivatives is underway, guided by docking studies of compound **4** to the PRMT1 crystal structure.

Materials and methods

Mice and cell culture

BALB/c mice were obtained from The Scripps Research Institute breeding colony. All animal protocols were in accordance with The Scripps Research Institute Institutional Animal Care and Use Committee policy. Th cells were isolated using magnetic bead selection (Miltenyi Biotech, Bergisch Gladbach, Germany). T cells were cultured in RPMI and stimulated with plate-bound anti-CD3 (1 $\mu g \cdot mL^{-1}$) (2C11; BioXCell) plus anti-CD28 (2 $\mu g \cdot mL^{-1}$) (PV1; BioXCell, West Lebanon, NH, USA), in the presence of IL-2 (NCI Biological Resources Branch). For Th1 skewing, 5 $ng \cdot mL^{-1}$ of recombinant IL-12 (14-8121; eBiosciences, San Diego, CA, USA) and 10 $\mu g \cdot mL^{-1}$ of anti-IL-4 (11B11; NCI Biological Resources Branch, Frederick, MD, USA) were added to the cell culture, and for Th2 skewing, 10 $ng \cdot mL^{-1}$ of recombinant IL-4 (14-8041; eBiosciences) and 10 $\mu g \cdot mL^{-1}$ of anti-IFN-γ (R4/GA2; BioXCell) were added to the cell culture. For stimulation with 4β-phorbol 12-myristate 13-acetate (PMA)/ionomycin, cells were incubated with 50 $ng \cdot mL^{-1}$ of PMA and 1 mM ionomycin (EMD Biosciences, Gibbstown, NJ, USA). Compounds were dissolved in dimethylsulfoxide. AMI-1 (AK Scientific, Mountain View, CA, USA and EMD Biosciences), Adox (Sigma, St Louis, MO, USA), MTA (Sigma) and sinefungin (Sigma) were solubilized in dimethylsulfoxide. Jurkat cells were grown in RPMI. 293T cells were grown in Dulbecco's modified Eagle's medium (DMEM). Proliferation assays were performed using the CellTiter 96 Aqueous One Solution Proliferation Assay reagent (Promega, Madison, WI, USA).

Plasmids, transfections and luciferase assays

GST–PRMT1 and GST–CARM1 vectors were described previously [1,34]. We thank Drs H. Herschman, S. Richard, M. Bedford and S. Clarke for GST–PRMT3, GST–PRMT6, GST–PRMT8 and GST–GAR vectors, respectively. Expression vectors for FLAG–PRMT1, HA–PRMT1, FLAG–NIP45 and IL-4 luciferase were described previously [7]. Transient transfection of 293T cells was performed using Fugene HD (Roche, Basel, Switzerland), according to the manufacturer's instructions. Jurkat cells were transfected using a BioRad electroporator (Hercules, CA, USA) (280 V, 975 μF). Thymidine kinase promoter-driven Renilla luciferase (TK-Renilla luciferase) was used as an internal control. Luciferase activity was determined using Promega's Dual Luciferase Kit.

ELISA

Th1 or Th2 cells (1×10^6 $cells \cdot mL^{-1}$) from day 7 cultures were stimulated with plate-bound anti-CD3 (1 $\mu g \cdot mL^{-1}$) for 24 h. IL-4 or IFN-γ protein levels in cell supernatants were measured using ELISA, as described previously (eBiosciences) [7].

In vitro methylation assays

Recombinant GST–PRMT1, GST–PRMT3, GST–PRMT4, GST–PRMT6, GST–PRMT8 and GST-GAR were prepared as described previously [21] and concentrated using a micron 10 filter device (Millipore, Billerica, MA, USA). Set7/9 (ALX-201-178) was purchased from Enzo Life Sciences. Methylation reactions were performed, as described previously, using recombinant histone 3 (12-357; Millipore), histone 4 (12-347; Millipore), or calf thymus histones (H4380; Sigma) [7]. The reactions were quantified by densitometry (IMAGEJ software, National Institutes of Health, Bethesda, MD, USA) and the IC_{50} values were calculated using linear regression.

Antibodies, immunoprecipitations and immunoblots

Whole-cell lysates were prepared using 1% Triton X-100 lysis buffer. For co-immunoprecipitation experiments, cell lysates were prepared in a lysis buffer containing 100 mM NaCl, 50 mM Tris (pH 7.5), 1 mM EDTA, 0.1% Triton X-100, 10 mM NaF, 1 mM phenylmethanesulfonyl fluoride and 1 mM vanadate. Immunoprecipitations were performed using anti-HA agarose (Sigma). The primary antibodies used in these studies were: anti HA–HRP (12CA5; Roche), anti-FLAG–HRP (M2; Sigma), anti-β-actin (ab8226; Abcam) and anti-histone 3 dimethylarginine 17 (07-214; Millipore).

Inhibitor reversibility assay

GST–PRMT1 bound to glutathione–agarose beads was incubated for 60 min on ice in the presence of 100 μM compounds. Samples were then washed three times with methylation reaction buffer (20 mm Tris, pH 8.0, 200 mM NaCl, 0.4 mM EDTA) containing either 100 μM inhibitor or dimethylsulfoxide. Samples were resuspended in methylation reaction buffer containing 100 μM inhibitor or dimethylsulfoxide, 1 μg of histones and 6 μM *S*-adenosyl-[methyl-^{3}H]methionine. The reactions were incubated for 90 min at room temperature and stopped with SDS sample buffer. Fluorography was performed as described previously [35].

Crosslinking

GST–PRMT1 (10 μg) was suspended in NaCl/P_i (PBS) containing 5 mM dithiothreitol, 100 μM inhibitor (sinefungin, AMI-1 or compound **4**) and 20 μM *S*-adenosyl-[methyl-^{3}H]methionine, and added to a 96-well plate

precooled on ice. Wells were exposed to short-wave UV light (UVP Inc. Model #UVGL-25, Upland, CA, USA) for 1 h. Fluorography was performed as described previously [8].

Synthesis

All air-sensitive and moisture-sensitive reactions were performed under nitrogen in oven-dried or flame-dried glassware. Unless stated otherwise, reagents and solvents were purchased from VWR, Acros, TCI America, or Aldrich, and were used without further purification. All experiments were monitored by TLC with visualization by exposure to UV light, iodine vapor, or a staining solution (5% phosphomolybdic acid in ethanol, anisaldehyde in EtOH, or aqueous $KMnO_4$) followed by heating. Flash chromatography was performed using SINGLE StEP pre-packed medium pressure liquid chromatographic columns (Thomson Instrument Company, Oceanside, CA, USA). Melting points were determined using a Barnstead Electrothermal 9300 capillary melt apparatus and are uncorrected. NMR spectra were recorded using an Inova-400 spectrometer (Varian, Palo Alto, CA, USA) (400 MHz for ^{1}H, 100 MHz for ^{13}C) in dimethylsulfoxide-d_6 solvent. Routine mass spectra were obtained using an Agilent 1100 (Santa Clara, CA, USA) (G1946D) electrospray ionization mass spectrometric detection with mobile phase composed of 9 : 1 CD_3CN : H_2O containing 0.1% CF_3CO_2H. GC/MS analyses were performed on an HP GCD-II (Model 5810) instrument. Elemental analyses were performed by Midwest MicroLab, LLC. High-resolution mass spectra were recorded at the MS facility at The Scripps Research Institute, La Jolla.

The synthetic steps are outlined in Fig. S1. In addition to *p*-methoxyaniline, the other four aromatic amines shown at the bottom of the figure were also tested and the resulting azo compounds were elaborated into candidate structures, the last of which proved to be as effective as compounds **1-5**, and will be the subject of further studies.

Compound 1

To a stirred solution of 4-methoxyaniline (665 mg, 5.40 mmol) in aqueous hydrochloric acid (30% v/v, 5.4 mL) was added dropwise a solution of sodium nitrite (401 mg, 5.83 mmol) in H_2O (1 mL) at 0 °C. The reaction mixture was stirred for 15 min or until a positive test (deep blue color) for nitrous acid on potassium iodide-starch test paper was observed. The clear yellowish solution of diazonium salt was used immediately for the subsequent coupling reaction. Note: if the arylamine did not dissolve well in aqueous acid, the reaction mixture was sonicated or gradually heated to 70 °C until a clear solution was obtained. The solution was then cooled to 0–5 °C in an ice bath.

6-Amino-1-naphtol-3-sulfonic acid (1.3 g, 5.40 mmol) was dissolved first in 5 M aqueous sodium hydroxide (5 mL) and then diluted with water (20 mL). This solution was added dropwise to a solution of the above diazonium chloride salt at 0 °C with stirring. Aqueous sodium hydroxide was added to maintain the mixture at pH 7, and the solution was stirred at 0 °C until a negative test on potassium iodide-starch test paper was observed. A fine brick-red solid precipitated and was isolated by several cycles of settling, decanting and dilution using pure water, followed by lyophilization, to give compound **1** in 70–80% yield. ^{1}H NMR (400 MHz, dimethylsulfoxide-d_6) δ 16.3 (s, 1H), 7.92 (d, J = 8.4 Hz, 1H), 7.63 (d, J = 9.2 Hz, 2H), 7.21 (s, 1H), 7.01 (d, J = 9.2 Hz, 2H), 6.71-6.63 (m, 2H), 3.78 (s, 3H). ^{13}C NMR (dimethylsulfoxide-d_6, spectrum acquired at 40 °C to aid solubility) δ 174.0, 157.1, 153.4, 143.4, 137.6, 136.9, 128.4, 127.6, 119.9, 119.5, 118.2, 114.6, 114.5, 109.7, 55.4. The compound appeared unchanged upon heating to 350 °C in a melting point capillary tube.

Compound 2

To a stirred suspension of compound **1** (3.36 g, 8.5 mmol) in methanol (72 mL) was added sodium carbonate (2.5 g, 24.5 mol) and 9-fluorenylmethyl chloroformate (Fmoc-Cl, 5.85 g, 22.7 mol) portionwise at room temperature. The reaction mixture was stirred for 24 h, after which 4 M HCl/dioxane (14 mL, 46 mol) was added and the suspension was stirred for 1 h. The solvent was removed on a rotary evaporator and the crude product was triturated with diethyl ether, and compound **2** was isolated as a red solid. ^{1}H NMR (200 MHz, dimethylsulfoxide-d_6) δ 16.2 (s, 1H), 10.2 (s, 1H), 8.17 (d, J = 8.8 Hz, 1H), 7.95 (d, J = 8.8 Hz, 2H), 7.80 (m, 5H), 7.60 (m, 1H), 7.39 (m, 5H), 7.08 (d, J = 8.8 Hz, 2H), 4.56 (d, J = 3 Hz, 2H), 4.37 (t, J = 3 Hz, 1H), 3.83 (s, 3H). ^{13}C (dimethylsulfoxide-d_6) δ 170.4, 158.5, 153.3, 143.9, 143.6, 142.8, 140.8, 137.6, 136.2, 127.7, 127.2, 125.2, 124.5, 120.3, 119.9, 119.1, 117.9, 115.6, 114.8, 66.0, 55.5, 46.6. The compound appeared unchanged upon heating to 350 °C in a melting point capillary tube.

Compound 3

To a stirred suspension of compound **2** (6.0 g, 10.0 mol) in dioxane (80 mL) was added triisopropylorthoformate (9.2 mL, 48 mol) at room temperature. The reaction mixture was stirred at 60 °C overnight, cooled to room temperature, filtered and the solid washed three times with CH_2Cl_2. The combined solutions were evaporated and the residue purified by column chromatography on silica gel [EtOAc/hexanes, 1:5 (v/v)] to give compound **3** as a red solid (5.2 g, 83%). R_f: 0.8 [EtOAc/hexanes, 1:2 (v/v)]; ^{1}H NMR (200 MHz, dimethylsulfoxide-d_6) δ 16.2 (s, 1H), 10.2 (s, 1H), 8.26 (d, J = 8.8 Hz, 1H), 7.96 (m, 3H), 7.77 (m, 5H), 7.60 (m, 6H), 7.39 (m, 4H), 7.07 (d, J = 8.8 Hz, 2H), 4.81 (m, 1H), 4.56 (d, J = 3 Hz, 2H), 4.37 (t, J = 3 Hz, 1H), 3.83 (s, 3H), 1.26 (d, J = 3Hz, 6H). ^{13}C (dimethylsulfoxide-d_6) δ 171.2,

159.2, 154.0, 144.6, 144.4, 143.5, 141.5, 138.3, 136.9, 128.4, 127.8, 125.8, 125.3, 120.9, 120.6, 119.9, 118.6, 116.3, 115.9, 66.7, 56.1, 55.5, 47.2, 27.7. The compound discolored at approximately 200 °C and partially sublimed at 250–255 °C, leaving a dark residue behind.

Compound 5

To a stirred solution of compound **3** (3.0 g, 4.7 mol) in dimethylformamide (8 mL) was added 4-methylpiperidine (722 μL, 6.11 mmol) at room temperature. After 2 h, the reaction mixture was partitioned between EtOAc and brine solution. The combined organic solution was washed with 1 M HCl to remove extra 4-methylpiperidine and then with water and brine, dried over anhydrous $MgSO_4$, filtered and concentrated. The crude product was purified by silica gel chromatography [EtOAc/hexanes, 1:5 (v/v)] to give the intermediate amine (**A** in Fig. S1) as a red solid (1.67 g, 86%). R_f: 0.4 [EtOAc/hexanes, 1:1 (v/v)]; ^{1}H NMR (200 MHz, $CDCl_3$) δ 8.26 (d, J = 8.4 Hz, 1H), 7.64 (m, 3H), 6.91 (m, 4H), 4.88 (m, 1H), 3.85 (s, 3H), 1.33 (d, 6H). LCMS $[M + H]^+$ 416.0.

A stirred suspension of compound **A** (114 mg, 0.274 mmol) in acetone (1.5 mL) was treated with cyanuric chloride (75.8 mg, 0.411 mmol) and saturated $NaHCO_3$ (34 μL) at room temperature. After 3 h, the reaction mixture was filtered and the crude product was purified on silica gel, eluting with EtOAc/hexanes (1:5, v/v) to give **5** as a red solid (127 mg, 83%) R_f: 0.8 [EtOAc/hexanes, 1:1 (v/v)]; ^{1}H NMR (200 MHz, dimethylsulfoxide-d_6) δ 16.3 (s, 1H), 11.6 (s, 1H), 8.37 (d, J = 8 Hz, 1H), 8.08 (s, 1H), 7.96 (d, J = 8 Hz, 1H), 7.87 (s, 1H), 7.76 (d, J = 8 Hz, 2H), 7.15 (d, J = 8 Hz, 2H), 4.61 (m, 1H), 3.82 (s, 3H), 1.21 (d, J = 3 Hz, 6H); LCMS $[M + H]^+$ 563.0.

Compound 4

To a stirred suspension of compound **5** (84.8 mg, 0.150 mmol) in 2-butanone (2 mL) was added sodium iodide (33.7 mg, 0.225 mmol) at room temperature. The reaction mixture was heated to 60 °C and allowed to stir overnight. The reaction mixture was then cooled to room temperature, filtered and washed with diethyl ether to provide compound **4** as a red solid (quant.). ^{1}H NMR (400 MHz, dimethylsulfoxide-d_6) δ 16.3 (s, 1H), 11.5 (s, 1H), 8.30 (d, J = 8 Hz, 1H), 8.07 (s, 1H), 7.81 (m, 2H), 7.52 (s, 1H), 7.11 (d, J = 7.4 Hz, 2H), 3.83 (s, 3H). The compound discolored when heated to 305–320 °C; melting was not evident up to 350 °C.

Acknowledgements

We thank Dr Sanja Arandjelovic for critical reading and review of the manuscript. This is manuscript # 20585 from TSRI. This work was partially supported by grants from NIAID AI067460-01 (K.A.M.), NIGMS GM085117 (K.A.M.), Skaggs Institute for Chemical Biology (M.G.F.), and the U.S. Department of Defense (W81XWH-05-1-0316) (M.G.F.). K.A.M is the recipient of an Arthritis Investigator Award and the Donald and Delia Baxter Foundation Young Career Scientist Award.

References

1 Lin WJ, Gary JD, Yang MC, Clarke S & Herschman HR (1996) The mammalian immediate-early TIS21 protein and the leukemia-associated BTG1 protein interact with a protein-arginine N-methyltransferase. *J Biol Chem* **271**, 15034–15044.

2 Bedford MT & Richard S (2005) Arginine methylation an emerging regulator of protein function. *Mol Cell* **18**, 263–272.

3 Krause CD, Yang ZH, Kim YS, Lee JH, Cook JR & Pestka S (2007) Protein arginine methyltransferases: evolution and assessment of their pharmaco logical and therapeutic potential. *Pharmacol Ther* **113**, 50–87.

4 Lee DY, Ianculescu I, Purcell D, Zhang X, Cheng X & Stallcup MR (2007) Surface-scanning mutational analysis of protein arginine methyltransferase 1: roles of specific amino acids in methyltransferase substrate specificity, oligomerization, and coactivator function. *Mol Endocrinol* **21**, 1381–1393.

5 Blanchet F, Cardona A, Letimier FA, Hershfield MS & Acuto O (2005) CD28 costimulatory signal induces protein arginine methylation in T cells. *J Exp Med* **202**, 371–377.

6 Richard S, Morel M & Cleroux P (2005) Arginine methylation regulates IL-2 gene expression: a role for protein arginine methyltransferase 5 (PRMT5). *Biochem J* **388**, 379–386.

7 Mowen KA, Schurter BT, Fathman JW, David M & Glimcher LH (2004) Arginine methylation of NIP45 modulates cytokine gene expression in effector T lymphocytes. *Mol Cell* **15**, 559–571.

8 Cheng D, Yadav N, King RW, Swanson MS, Weinstein EJ & Bedford MT (2004) Small molecule regulators of protein arginine methyltransferases. *J Biol Chem* **279**, 23892–23899.

9 Williams-Ashman HG, Seidenfeld J & Galletti P (1982) Trends in the biochemical pharmacology of 5′-deoxy-5′-methylthioadenosine. *Biochem Pharmacol* **31**, 277–288.

10 Osborne TC, Obianyo O, Zhang X, Cheng X & Thompson PR (2007) Protein arginine methyltransferase 1: positively charged residues in substrate peptides distal to the site of methylation are important for substrate binding and catalysis. *Biochemistry* **46**, 13370–13381.

11 Clarke SG (2006) Inhibition of mammalian protein methyltransferases by 5′-methylthioadenosine (MTA): a mechanism of action of dietary SAMe? In *The Enzymes: Protein Methyltransferases* (Clarke SG, ed.), pp. 467–486. Elsevier, London.
12 Spannhoff A, Heinke R, Bauer I, Trojer P, Metzger E, Gust R, Schule R, Brosch G, Sippl W & Jung M (2007) Target-based approach to inhibitors of histone arginine methyltransferases. *J Med Chem* **50**, 2319–2325.
13 Spannhoff A, Machmur R, Heinke R, Trojer P, Bauer I, Brosch G, Schule R, Hanefeld W, Sippl W & Jung M (2007) A novel arginine methyltransferase inhibitor with cellular activity. *Bioorg Med Chem Lett* **17**, 4150–4153.
14 Mai A, Cheng D, Bedford MT, Valente S, Nebbioso A, Perrone A, Brosch G, Sbardella G, De Bellis F, Miceli M *et al.* (2008) epigenetic multiple ligands: mixed histone/protein methyltransferase, acetyltransferase, and class III deacetylase (sirtuin) inhibitors. *J Med Chem* **51**, 2279–2290.
15 Mai A, Valente S, Cheng D, Perrone A, Ragno R, Simeoni S, Sbardella G, Brosch G, Nebbioso A, Conte M *et al.* (2007) Synthesis and biological validation of novel synthetic histone/protein methyltransferase inhibitors. *ChemMedChem* **2**, 987–991.
16 Rho J, Choi S, Seong YR, Cho WK, Kim SH & Im DS (2001) Prmt5, which forms distinct homo-oligomers, is a member of the protein-arginine methyltransferase family. *J Biol Chem* **276**, 11393–11401, doi: 10.1074/jbc.M008660200, M008660200 [pii].
17 Zhang X & Cheng X (2003) Structure of the predominant protein arginine methyltransferase PRMT1 and analysis of its binding to substrate peptides. *Structure* **11**, 509–520.
18 Iberg AN, Espejo A, Cheng D, Kim D, Michaud-Levesque J, Richard S & Bedford MT (2008) Arginine methylation of the histone H3 tail impedes effector binding. *J Biol Chem* **283**, 3006–3010, doi: 10.1074/jbc.C700192200, C700192200 [pii].
19 Glimcher LH & Murphy KM (2000) Lineage commitment in the immune system: the T helper lymphocyte grows up. *Genes Dev* **14**, 1693–1711.
20 Lawson BR, Manenkova Y, Ahamed J, Chen X, Zou JP, Baccala R, Theofilopoulos AN & Yuan C (2007) Inhibition of transmethylation down-regulates CD4 T cell activation and curtails development of autoimmunity in a model system. *J Immunol* **178**, 5366–5374.
21 Hodge MR, Chun HJ, Rengarajan J, Alt A, Lieberson R & Glimcher LH (1996) NF-AT-Driven interleukin-4 transcription potentiated by NIP45. *Science* **274**, 1903–1905.
22 Bedford MT (2007) Arginine methylation at a glance. *J Cell Sci* **120**, 4243–4246.
23 Skillman AG, Maurer KW, Roe DC, Stauber MJ, Eargle D, Ewing TJ, Muscate A, Davioud-Charvet E, Medaglia MV, Fisher RJ *et al.* (2002) A novel mechanism for inhibition of HIV-1 reverse transcriptase. *Bioorg Chem* **30**, 443–458, doi: S0045206802005023 [pii].
24 Ragno R, Simeoni S, Castellano S, Vicidomini C, Mai A, Caroli A, Tramontano A, Bonaccini C, Trojer P, Bauer I *et al.* (2007) Small molecule inhibitors of histone arginine methyltransferases: homology modeling, molecular docking, binding mode analysis, and biological evaluations. *J Med Chem* **50**, 1241–1253.
25 Feng Y, Xie N, Wu J, Yang C & Zheng YG (2009) Inhibitory study of protein arginine methyltransferase 1 using a fluorescent approach. *Biochem Biophys Res Commun* **379**, 567–572, doi: 10.1016/j.bbrc.2008.12.119, S0006-291X(08)02522-9 [pii].
26 Osborne T, Roska RL, Rajski SR & Thompson PR (2008) In situ generation of a bisubstrate analogue for protein arginine methyltransferase 1. *J Am Chem Soc* **130**, 4574–4575, doi: 10.1021/ja077104v.
27 Allan M, Manku S, Therrien E, Nguyen N, Styhler S, Robert MF, Goulet AC, Petschner AJ, Rahil G, Robert Macleod A *et al.* (2009) N-Benzyl-1-heteroaryl-3-(trifluoromethyl)-1H-pyrazole-5-carboxamides as inhibitors of co-activator associated arginine methyltransferase 1 (CARM1). *Bioorg Med Chem Lett* **19**, 1218–1223, doi: 10.1016/j.bmcl.2008.12.075, S0960-894X(08)01600-4 [pii].
28 Huynh T, Chen Z, Pang S, Geng J, Bandiera T, Bindi S, Vianello P, Roletto F, Thieffine S, Galvani A *et al.* (2009) Optimization of pyrazole inhibitors of Coactivator Associated Arginine Methyltransferase 1 (CARM1). *Bioorg Med Chem Lett* **19**, 2924–2927, doi: 10.1016/j.bmcl.2009.04.075, S0960-894X(09)00569-1 [pii].
29 Purandare AV, Chen Z, Huynh T, Pang S, Geng J, Vaccaro W, Poss MA, Oconnell J, Nowak K & Jayaraman L (2008) Pyrazole inhibitors of coactivator associated arginine methyltransferase 1 (CARM1). *Bioorg Med Chem Lett* **18**, 4438–4441, doi: 10.1016/j.bmcl.2008.06.026, S0960-894X(08)00675-6 [pii].
30 Mahler M, Fritzler MJ & Bluthner M (2005) Identification of a SmD3 epitope with a single symmetrical dimethylation of an arginine residue as a specific target of a subpopulation of anti-Sm antibodies. *Arthritis Res Ther* **7**, R19–R29, doi: 10.1186/ar1455, ar1455 [pii].
31 Mahler M, Raijmakers R, Dahnrich C, Bluthner M & Fritzler MJ (2005) Clinical evaluation of autoantibodies to a novel PM/Scl peptide antigen. *Arthritis Res Ther* **7**, R704–R713, doi: 10.1186/ar1729, ar1729 [pii].
32 Covic M, Hassa PO, Saccani S, Buerki C, Meier NI, Lombardi C, Imhof R, Bedford MT, Natoli G & Hottiger MO (2005) Arginine methyltransferase CARM1 is a promoter-specific regulator of NF-kappaB-dependent gene expression. *EMBO J* **24**, 85–96.

33 Brahms H, Raymackers J, Union A, de Keyser F, Meheus L & Luhrmann R (2000) The C-terminal RG dipeptide repeats of the spliceosomal Sm proteins D1 and D3 contain symmetrical dimethylarginines, which form a major B-cell epitope for anti-Sm autoantibodies. *J Biol Chem* **275**, 17122–17129, doi: 10.1074/jbc.M000300200, M000300200 [pii].

34 Chen D, Ma H, Hong H, Koh SS, Huang SM, Schurter BT, Aswad DW & Stallcup MR (1999) Regulation of transcription by a protein methyltransferase. *Science* **284**, 2174–2177.

35 Mowen KA, Tang J, Zhu W, Schurter BT, Shuai K, Herschman HR & David M (2001) Arginine methylation of STAT1 modulates IFNalpha/beta-induced transcription. *Cell* **104**, 731–741.

Supporting information

The following supplementary material is available:
Fig. S1. Synthesis of new PRMT inhibitors.

This supplementary material can be found in the online version of this article.

Please note: As a service to our authors and readers, this journal provides supporting information supplied by the authors. Such materials are peer-reviewed and may be re-organized for online delivery, but are not copy-edited or typeset. Technical support issues arising from supporting information (other than missing files) should be addressed to the authors.